Available online at www.sciencedirect.com
ScienceDirect
Journal of the European Ceramic Society 27 (2007) 273–277
www.elsevier.com/locate/jeurceramsoc

Oxygen nonstoichiometry in $Pr_{1-x}Sr_xCo_{0.2}B_{0.8}O_{3-\delta}$ (B = Mn, Fe, $x = 0.2, 0.4$) perovskite oxides

G.Ch. Kostogloudis [1], Ch. Ftikos *

Laboratory of Inorganic Materials Technology, Department of Chemical Engineering, National Technical University of Athens, 9 Heroon Polytechniou Str., Zografou Campus, GR-157 80 Athens, Greece

Received 24 October 2005; received in revised form 13 February 2006; accepted 27 February 2006
Available online 18 May 2006

Abstract

Thermogravimetric analysis was applied to the study of oxygen nonstoichiometry of perovskite oxides of the compositions $Pr_{0.8}Sr_{0.2}Co_{0.2}Mn_{0.8}O_{3-\delta}$ and $Pr_{1-x}Sr_xCo_{0.2}Fe_{0.8}O_{3-\delta}$ ($x = 0.2, 0.4$). The measurements were performed in the temperature range from room temperature to 1200 °C in various atmospheres: oxygen, air and argon. The recorded weight loss corresponds to the loss of lattice oxygen. The magnitude of oxygen loss increased and the temperature at which oxygen loss became significant decreased with increasing Sr content. The loss of lattice oxygen became more significant as the oxygen partial pressure decreased. For the same pO_2 and level of Sr doping, the Fe-containing composition became more easily oxygen deficient than the corresponding Mn-containing one, suggesting that Fe is more resistant to oxidation from the trivalent to the tetravalent state than Mn. Electrical conductivity measurements, performed in air, showed that the temperature ranges at which conductivity decrease was observed, correspond fairly well with those ranges where weight loss was detected.

Keywords: Perovskites; Fuel cells; Thermal properties; (Pr,Sr)(Co,Mn)O_3

1. Introduction

Ceramic oxides with the perovskite structure and composition $RE_{1-x}Sr_xCo_{1-y}B_yO_{3-\delta}$ (RE = rare earth, B = transition metal) have been widely investigated in recent years, due to their mixed electronic–ionic conducting behavior at high temperatures.[1,2] The appearance of electronic and oxide-ion conductivity in these perovskites is due to the existence, in their lattice, of B^{4+} small polarons and oxygen vacancies, respectively. These defects are formed for charge compensation reasons, when the acceptor dopant Sr^{2+} is substituted for RE^{3+} in the perovskite lattice. The mixed conducting capability of these oxides makes them attractive candidate materials for several applications, such as, solid oxide fuel cell cathodes, oxygen separation membranes and membrane reactors.[1] Selected low Co-containing perovskite oxide compositions are considered promising.[2] Moreover, it has been reported[3] that, among perovskites with different rare earth cations at the A-site, those incorporating Pr^{3+}, exhibited the highest electrical conductivity and maintained the lowest overpotential values.

The oxide-ion conductivity of perovskite oxides is directly dependent on the extent at which oxygen vacancies are formed in their lattice. Therefore, the measurement of oxygen deficiency can give valuable information that can assist in the evaluation of these oxides for potential application.

The purpose of this work was the application of thermogravimetric analysis to the study of oxygen nonstoichiometry of perovskite oxides of the compositions $Pr_{0.8}Sr_{0.2}Co_{0.2}Mn_{0.8}O_{3-\delta}$ and $Pr_{1-x}Sr_xCo_{0.2}Fe_{0.8}O_{3-\delta}$ ($x = 0.2, 0.4$). Weight loss measurements were performed on these oxides in various atmospheres: oxygen, air and argon. The results obtained from these thermogravimetric measurements were supplemented by electrical conductivity measurements.

2. Experimental

Ceramic oxide powders of the compositions $Pr_{0.8}Sr_{0.2}Co_{0.2}Mn_{0.8}O_{3-\delta}$ and $Pr_{1-x}Sr_xCo_{0.2}Fe_{0.8}O_{3-\delta}$ ($x = 0.2, 0.4$) were prepared by the amorphous citrate process.[4] Pr_6O_{11}, and

* Corresponding author. Tel.: +30 210 772 3243; fax: +30 210 772 3244.
E-mail address: chftikos@orfeas.chemeng.ntua.gr (Ch. Ftikos).
[1] Present address: Ministry of National Defence, Papagou Campus, Holargos, Greece.

0955-2219/$ – see front matter © 2006 Elsevier Ltd. All rights reserved.
doi:10.1016/j.jeurceramsoc.2006.02.044

Table 1
Phase symmetry, lattice parameters, unit cell volume and pseudo-cubic lattice constant of the perovskite oxides of this study

Oxide	Phase symmetry	a (Å)	b (Å)	c (Å)	Volume (Å^3)	a' (Å)
$Pr_{0.8}Sr_{0.2}Co_{0.2}Mn_{0.8}O_{3-\delta}$	Orthorhombic	5.4626	5.4620	7.7274	230.59	3.8630
$Pr_{0.8}Sr_{0.2}Co_{0.2}Fe_{0.8}O_{3-\delta}$	Orthorhombic	5.4554	5.4736	7.7439	231.2	3.8666
$Pr_{0.6}Sr_{0.4}Co_{0.2}Fe_{0.8}O_{3-\delta}$	Orthorhombic	5.4469	5.4539	7.7080	229.0	3.8540

$(CH_3COO)_2Co{\cdot}4H_2O$ were dissolved in nitric acid, while $Sr(NO_3)_2$, $(CH_3COO)_2Mn{\cdot}4H_2O$ and $Fe(NO_3)_3{\cdot}9H_2O$ were dissolved in distilled water, all in the correct molar proportions. The solutions were mixed together and an aqueous solution containing 1.5 mol of citric acid per mole of metal was added. The final solution was evaporated over a burner flame until a powder was obtained. The powder was calcined in air at 1100 °C for 15 h and then cooled at a slow rate (1 °C/min), with the aim to obtain the equilibrium oxygen content. Wet milling with acetone was then performed, using zirconia balls as the grinding medium.

The specimens for the XRD study were fired at 1300 °C for 15 h and then cooled at a slow rate (1 °C/min), with the aim to obtain the equilibrium oxygen content. The TGA measurements performed showed that the samples were oxygen stoichiometric at room temperatures. The crystal structure and the determination of the lattice parameters of the oxides were performed at room temperature by X-ray powder diffraction (XRD) on a SIEMENS diffractometer using Cu Kα radiation. The diffractometer was operated at 40 kV and 30 mA. The XRD data were collected by step scanning in the range $10 \leq 2\theta \leq 80$ in increments of 0.02° 2θ. The lattice parameters were determined using a least squares unit cell refinement computer program (LSUCR).

Weight loss measurements were performed on the prepared oxides (sample weight: 40 mg) by thermogravimetric analysis (TGA), using Al_2O_3 standard, in the temperature range from room temperature to 1200 °C (STA 409, Netzsch). In order to achieve thermodynamic equilibrium, a relatively slow heating rate of 3 °C/min was used. The weight gain upon cooling agreed fairly well with the results obtained during heating. The TGA measurements were performed in various atmospheres: oxygen, air and argon.

The samples for the electrical conductivity measurements were prepared by uniaxial pressing at 250 MPa, and sintered at 1300 °C for 15 h in air. A slow rate of 1 °C min^{-1} was used during heating and cooling. The sample densities were above 95% of the theoretical values, in all cases. The electrical conductivity was measured in air by the standard four point DC method upon heating in the temperature range 25–1000 °C.

3. Results

3.1. Crystal structure

The X-ray powder diffraction patterns of the oxides showed that single phase materials were obtained in all cases. The patterns were indexed on the basis of a distorted perovskite structure with orthorhombic $GdFeO_3$-type[5] symmetry (space group *Pbnm*). Each unit cell consists of four units, and has the approximate dimensions $\sqrt{2}a_p \times \sqrt{2}a_p \times 2a_p$, where a_p is the lattice parameter of the ideal cubic unit cell. The calculated lattice parameters and the volume of the unit cell are shown in Table 1.

The pseudo-cubic lattice constant a', defined as:

$$a' = \left(\frac{V}{z}\right)^{1/3} \quad (1)$$

where $z = 4$ for the orthorhombic perovskite oxides of this study, is also shown in Table 1. As can be seen, a' decreases on increasing Sr content in $Pr_{1-x}Sr_xCo_{0.2}Fe_{0.8}O_{3-\delta}$, and also when substituting Mn for Fe at the B-site of $Pr_{0.8}Sr_{0.2}Co_{0.2}B_{0.8}O_{3-\delta}$ oxides. The change in the size of a' depends on factors such us the difference in the ionic radius of the dopant cation (Sr^{2+}) in relation to the host cation (Pr^{3+}), as well as the ionic radii difference between the transition metals at the B-site. The introduction of Sr^{2+} cation on a Pr^{3+} lattice position is electronically compensated by the oxidation of the transition metal from the trivalent to the tetravalent state. In Table 2, the ionic radii of the cations involved in this study are shown, according to Shannon.[6] In $Pr_{1-x}Sr_xCo_{0.2}Fe_{0.8}O_{3-\delta}$, the smaller size of Co^{4+} and Fe^{4+} cations compared to Co^{3+} and Fe^{3+} cations, respectively, leads to the decrease of a' on increasing Sr^{2+} substitution.

If we consider a fixed composition at the A-site, as in the case of $Pr_{0.8}Sr_{0.2}Co_{0.2}B_{0.8}O_{3-\delta}$ (B = Mn, Fe), inspection of the transition metal ionic radii (Table 2) reveals that while the trivalent Mn and Fe ions have equal sizes, the Mn^{4+} cation is smaller than the Fe^{4+} cation. Therefore, the substitution of Mn for Fe in these Sr-doped perovskite oxides, where Mn^{4+} and Fe^{4+} cations are expected to be present, causes the decrease of the size of the unit cell, and a' decreases.

3.2. Oxygen nonstoichiometry

The results of the weight loss of the oxides with compositions $Pr_{0.8}Sr_{0.2}Co_{0.2}Mn_{0.8}O_{3-\delta}$, $Pr_{0.8}Sr_{0.2}Co_{0.2}Fe_{0.8}O_{3-\delta}$ and $Pr_{0.6}Sr_{0.4}Co_{0.2}Fe_{0.8}O_{3-\delta}$, measured upon heating in air, are shown in Fig. 1. This weight loss was due to a partial

Table 2
Ionic radii of several cations, and their coordination number (CN) in the perovskite lattice[6]

Cation	Ionic radius (Å)
Pr^{3+} (CN = 12)	1.30
Sr^{2+} (CN = 12)	1.44
Co^{3+} (CN = 6)	0.545
Co^{4+} (CN = 6)	0.53
Mn^{3+} (CN = 6)	0.645
Mn^{4+} (CN = 6)	0.530
Fe^{3+} (CN = 6)	0.645
Fe^{4+} (CN = 6)	0.585

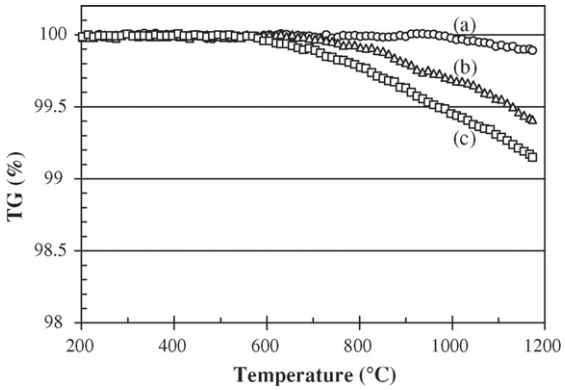

Fig. 1. TG weight loss vs. temperature for the compositions: (a) $Pr_{0.8}Sr_{0.2}Co_{0.2}Mn_{0.8}O_{3-\delta}$, (b) $Pr_{0.8}Sr_{0.2}Co_{0.2}Fe_{0.8}O_{3-\delta}$ and (c) $Pr_{0.6}Sr_{0.4}Co_{0.2}Fe_{0.8}O_{3-\delta}$ in air.

loss of lattice oxygen, so that the oxygen stoichiometry (3-δ) decreased with increasing temperature.[7,8] Between the compositions with the same level of Sr doping (20 mol%), the Fe-containing oxide showed a greater tendency for oxygen loss than the Mn-containing oxide. Also, the increase of Sr content in the ferrite oxides resulted in an increase of the magnitude of oxygen loss, in agreement with literature.[7,9] Moreover, the temperature at which the weight loss became significant decreased as the oxide showed a greater tendency to be oxygen nonstoichiometric.

Figs. 2 and 3 show the weight loss of $Pr_{0.8}Sr_{0.2}Co_{0.2}Mn_{0.8}O_{3-\delta}$ and $Pr_{0.8}Sr_{0.2}Co_{0.2}Fe_{0.8}O_{3-\delta}$, respectively, in different atmospheres: oxygen, air and argon. As can be seen, the oxygen partial pressure greatly influenced both the magnitude of the oxygen loss and the onset temperature at which this loss became significant. For both oxides, the decrease of pO_2 resulted in greater weight loss and reduction of its onset temperature. In oxygen atmosphere, $Pr_{0.8}Sr_{0.2}Co_{0.2}Mn_{0.8}O_{3-\delta}$ showed no oxygen loss in the whole examined temperature range, whereas $Pr_{0.8}Sr_{0.2}Co_{0.2}Fe_{0.8}O_{3-\delta}$ started to lose oxygen above 900 °C. In argon atmosphere and for both oxides, oxygen loss commenced at about 400 °C and was approximately the same above that temperature.

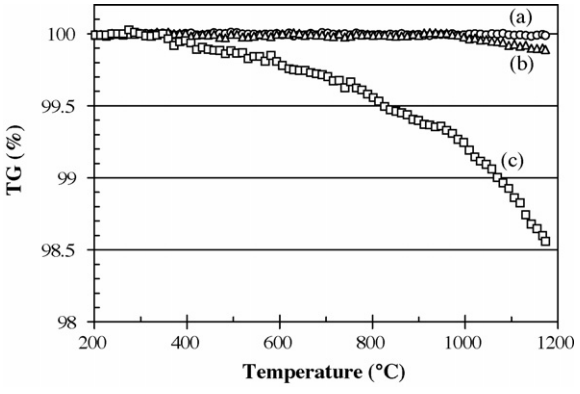

Fig. 2. TG weight loss vs. temperature for the composition $Pr_{0.8}Sr_{0.2}Co_{0.2}Mn_{0.8}O_{3-\delta}$ in: (a) oxygen, (b) air and (c) argon atmosphere.

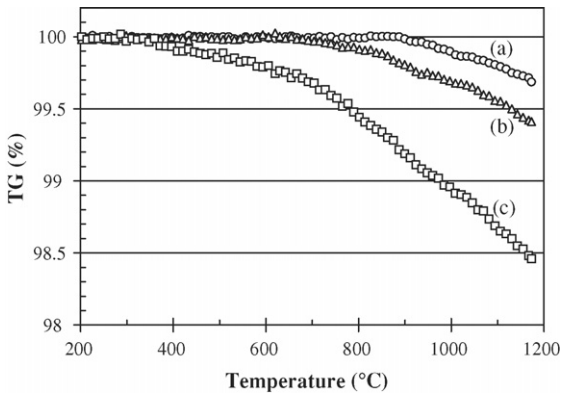

Fig. 3. TG weight loss vs. temperature for the composition $Pr_{0.8}Sr_{0.2}Co_{0.2}Fe_{0.8}O_{3-\delta}$ in: (a) oxygen, (b) air and (c) argon atmosphere.

$La_{0.6}Sr_{0.4}Co_{0.2}Fe_{0.8}O_{3-\delta}$ is essentially oxygen stoichiometric ($\delta = 0$) at room temperature, in air, as shown by iodometric titration,[7] and the same behavior is expected for $Pr_{0.6}Sr_{0.4}Co_{0.2}Fe_{0.8}O_{3-\delta}$. This composition showed the greatest tendency to lose oxygen among the oxides of this study. Therefore, it can be inferred that the other two oxides examined, should also be oxygen stoichiometric at room temperature in air. This reference point, combined with the weight loss measurements taken in air upon heating, made possible to determine the oxygen stoichiometry as a function of temperature. The results of these calculations are shown in Fig. 4. Oxygen deficiency was more significant for the Fe-containing compositions and increased with increasing Sr content. $Pr_{0.8}Sr_{0.2}Co_{0.2}Mn_{0.8}O_{3-\delta}$ was oxygen stoichiometric up to about 1000 °C, while the onset temperature at which the ferrite oxides started to become oxygen deficient was about 750 and 600 °C for $Pr_{0.8}Sr_{0.2}Co_{0.2}Fe_{0.8}O_{3-\delta}$ and $Pr_{0.6}Sr_{0.4}Co_{0.2}Fe_{0.8}O_{3-\delta}$, respectively.

3.3. Electrical conductivity

The logarithm of electrical conductivity versus reciprocal temperature in air is shown in Fig. 5. The electronic conductivity of the oxides of this study can be described by the small polaron hopping conductivity model.[10,11] The conductivity of the Mn-containing oxide increased up to 1000 °C. The Fe-containing

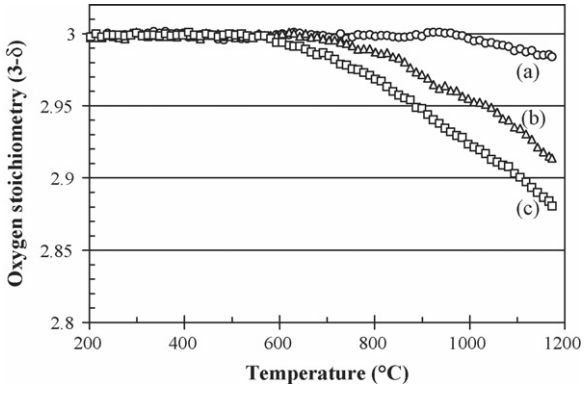

Fig. 4. Oxygen stoichiometry as a function of temperature for the compositions: (a) $Pr_{0.8}Sr_{0.2}Co_{0.2}Mn_{0.8}O_{3-\delta}$, (b) $Pr_{0.8}Sr_{0.2}Co_{0.2}Fe_{0.8}O_{3-\delta}$ and (c) $Pr_{0.6}Sr_{0.4}Co_{0.2}Fe_{0.8}O_{3-\delta}$ in air.

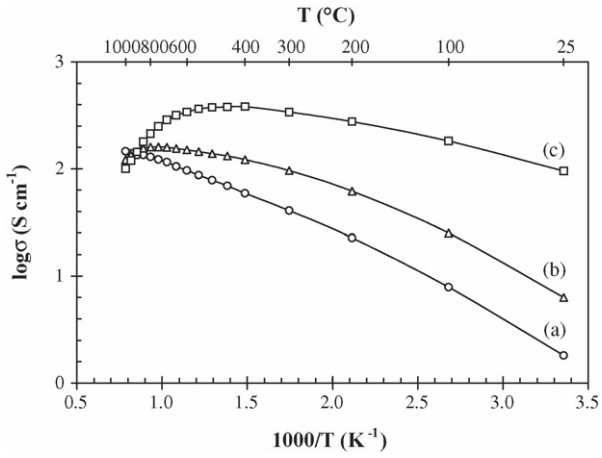

Fig. 5. Logarithm of electrical conductivity vs. reciprocal temperature for the compositions: (a) $Pr_{0.8}Sr_{0.2}Co_{0.2}Mn_{0.8}O_{3-\delta}$, (b) $Pr_{0.8}Sr_{0.2}Co_{0.2}Fe_{0.8}O_{3-\delta}$ and (c) $Pr_{0.6}Sr_{0.4}Co_{0.2}Fe_{0.8}O_{3-\delta}$ in air.

Table 3
Activation energies for the electrical conductivity of the oxides of this study, through the small polaron hopping mechanism

Oxide	Temperature range (°C)	E_a (kJ/mol)
$Pr_{0.8}Sr_{0.2}Co_{0.2}Mn_{0.8}O_{3-\delta}$	25–1000	17.2
$Pr_{0.8}Sr_{0.2}Co_{0.2}Fe_{0.8}O_{3-\delta}$	25–750	15.2
$Pr_{0.6}Sr_{0.4}Co_{0.2}Fe_{0.8}O_{3-\delta}$	25–550	9.8

oxides exhibited a maximum, above which, the conductivity decreased. This maximum was located at about 750 and 550 °C, for the ferrite compositions with 20 and 40 mol% Sr, respectively. The temperatures of the conductivity maxima coincide fairly well with the temperatures where the oxygen loss became significant in the TGA measurements. Therefore, the decrease of conductivity at high temperatures for $Pr_{1-x}Sr_xCo_{0.2}Fe_{0.8}O_{3-\delta}$ can be attributed to the decrease of its oxygen content.

The temperature dependence of electrical conductivity through the small polaron hopping mechanism is expressed by

$$\sigma = \frac{A}{T}\exp\left(-\frac{E_a}{kT}\right) \quad (2)$$

The slope of the $\log \sigma T$ versus $1/T$ line gives the activation energy, E_a. The values of E_a are given in Table 3, as calculated for the temperature ranges indicated, where the oxides showed semiconducting behavior and below the point where they start to loose oxygen. As can be seen, the activation energy decreases on increasing Sr content in $Pr_{1-x}Sr_xCo_{0.2}Fe_{0.8}O_{3-\delta}$, and increases when substituting Mn for Fe at the B-site of $Pr_{0.8}Sr_{0.2}Co_{0.2}B_{0.8}O_{3-\delta}$ oxides. This is the opposite behavior than that of the electrical conductivity (Fig. 5), as expected.

4. Discussion

The oxygen nonstoichiometry and electrical properties of $Pr_{1-x}Sr_xCo_{0.2}B_{0.8}O_{3-\delta}$ (B = Mn, Fe) depend on the composition, temperature and oxygen partial pressure. It is of interest, therefore, to consider the defect chemistry of $Pr_{1-x}Sr_xCo_{0.2}B_{0.8}O_{3-\delta}$ before we examine how the above factors influence its properties.

The composition $Pr_{1-x}Sr_xBO_{3-\delta}$ (B = Mn, Fe, Co) will be considered for simplicity. The substitution of Sr^{2+} for Pr^{3+} in $PrBO_3$ is electronically compensated by the oxidation of B^{3+} cations to B^{4+}:

$$PrBO_3 \xrightarrow{SrO} Pr^{\times}_{1-x}Sr'_xB^{\times}_{1-x}B^{\bullet}_xO_3 \quad (3)$$

and/or the formation of oxygen vacancies ($V_O^{\bullet\bullet}$):

$$Pr^{\times}_{1-x}Sr'_xB^{\times}_{1-x}B^{\bullet}_xO_3 \leftrightarrow Pr^{\times}_{1-x}Sr'_xB^{\times}_{1-x+2\delta}B_{x-2\delta}{}^{\bullet}O_{3-\delta}[\delta V_O^{\bullet\bullet}] + \frac{\delta}{2}O_2 \quad (4)$$

where according to Kröger-Vink notation, $Pr^{\times}$ and $B^{\times}$ are Pr^{3+} and B^{3+} cations, respectively, on regular sites, Sr' is a Sr^{2+} cation on a Pr^{3+} lattice position and $B^{\bullet}$ is a B^{4+} cation on a B^{3+} position in the perovskite lattice. When the temperature increases, or the pO_2 decreases, the equilibrium of Eq. (4) shifts to the right. As a result, oxygen vacancies ($V_O^{\bullet\bullet}$) are formed, at the expense of two B^{4+} cations to B^{3+} for each $V_O^{\bullet\bullet}$. Therefore, when temperature increases, the loss of lattice oxygen takes place, as recorded by the TGA measurements. The decrease of the concentration of the electronic charge carriers (B^{4+} small polarons), resulting from the oxygen loss, caused the electrical conductivity decrease, observed at high temperatures. Also, when the oxygen partial pressure decreases, the oxygen loss is enhanced and occurs from lower temperatures.

For the oxides of this study, two different transition metals are located at the B-site (Co-Mn or Co-Fe). These metals exist in the lattice in the trivalent and tetravalent states, and the relative concentration of each valence state is different for each metal. For a fixed Sr^{2+} content, and constant temperature and pO_2, the concentration of each valence state depends on the relative reduction/oxidation stability of the transition metal involved. According to the TGA measurements of this study, between the compositions $Pr_{0.8}Sr_{0.2}Co_{0.2}Mn_{0.8}O_{3-\delta}$ and $Pr_{0.8}Sr_{0.2}Co_{0.2}Fe_{0.8}O_{3-\delta}$, the Fe-containing one showed a greater oxygen loss. This observation is consistent with the results reported by Zhang et al.,[12] based on oxygen desorption measurements. The fact that ionic compensation became more prevalent in $Pr_{0.8}Sr_{0.2}Co_{0.2}Fe_{0.8}O_{3-\delta}$ than in $Pr_{0.8}Sr_{0.2}Co_{0.2}Mn_{0.8}O_{3-\delta}$, suggests that Fe is more resistant to oxidation from the trivalent to the tetravalent state than Mn.

When the concentration of the A-site acceptor dopant (Sr^{2+}) is increased, the relative importance of the compensation mechanism described by Eq. (4) increases over that described by Eq. (3).[13,14] As a result, the magnitude of the oxygen loss increases and the temperature at which this loss becomes significant decreases with increasing Sr content. Thus, the concentration of Sr^{2+} in the perovskite oxide controls the thermal stability of the lattice oxygen, in agreement with oxygen adsorption/desorption results reported in the literature.[15]

5. Conclusions

The oxides $Pr_{0.8}Sr_{0.2}Co_{0.2}Mn_{0.8}O_{3-\delta}$ and $Pr_{1-x}Sr_xCo_{0.2}Fe_{0.8}O_{3-\delta}$ ($x = 0.2$, 0.4) of this study have an orthorhombic $GdFeO_3$-type structure (space group *Pbnm*). The weight loss of the above compositions, recorded by TGA, corresponds to the loss of lattice oxygen. The results obtained from the Fe-containing compositions, in air, revealed that the magnitude of the oxygen loss increased and the onset temperature at which oxygen loss became significant decreased with increasing Sr content. The atmosphere influenced the measured weight loss. The thermogravimetric measurements on $Pr_{0.8}Sr_{0.2}Co_{0.2}B_{0.8}O_{3-\delta}$ (B = Mn, Fe) showed that the loss of lattice oxygen became more significant as the oxygen partial pressure decreased. For the same pO_2 and the same level of Sr doping ($x = 0.2$), the Fe-containing composition became more easily oxygen deficient than the corresponding Mn-containing one, suggesting that Fe is more resistant to oxidation from the trivalent to the tetravalent state than Mn. However, in argon atmosphere the oxygen loss recorded was approximately the same for the two compositions, $Pr_{0.8}Sr_{0.2}Co_{0.2}Mn_{0.8}O_{3-\delta}$ and $Pr_{0.8}Sr_{0.2}Co_{0.2}Fe_{0.8}O_{3-\delta}$. The results obtained from these thermogravimetric measurements were supplemented by electrical conductivity measurements. It was shown that the temperature ranges at which conductivity decrease was observed, correspond fairly well with those ranges where weight loss was detected.

References

1. Anderson, H. U., *Solid State Ionics*, 1992, **52**, 33.
2. Steele, B. C. H., *J. Power Sources*, 1994, **49**, 1.
3. Ishihara, T., Kudo, T., Matsuda, H. and Takita, Y., *J. Electrochem. Soc.*, 1995, **142**, 1519.
4. Blank, D. H. A., Kruidhof, H. and Flokstra, J., *J. Phys. D*, 1988, **21**, 226.
5. Geller, S., *J. Chem. Phys.*, 1956, **24**, 1236.
6. Shannon, R. D., *Acta Crystallogr.*, 1976, **A32**, 751.
7. Stevenson, J. W., Armstrong, T. R., Carneim, R. D., Pederson, L. R. and Weber, W. J., *J. Electrochem. Soc.*, 1996, **143**, 2722.
8. Tai, L.-W., Nastrallah, M. M., Anderson, H. U., Sparlin, D. M. and Sehlin, S. R., *Solid State Ionics*, 1995, **76**, 259.
9. Tai, L.-W., Nastrallah, M. M., Anderson, H. U., Sparlin, D. M. and Sehlin, S. R., *Solid State Ionics*, 1995, **76**, 273.
10. Cox, P. A., *The Electronic Structure and Chemistry of Solids*. Oxford University Press, Oxford, 1987.
11. Kostogloudis, G. Ch., Fertis, P. and Ftikos, Ch., *Solid State Ionics*, 1999, **118**, 241.
12. Zhang, H. M., Yamazoe, N. and Teraoka, Y., *J. Mater. Sci. Lett.*, 1989, **8**, 995.
13. Petrov, A. N., Kononchuk, O. F., Andreev, A. V., Cherepanov, V. A. and Kofstad, P., *Solid State Ionics*, 1995, **80**, 189.
14. Kostogloudis, G. Ch., Vasilakos, N. and Ftikos, Ch., *Solid State Ionics*, 1998, **106**, 207.
15. Zhang, H. M., Shimizu, Y., Teraoka, Y., Miura, N. and Yamazoe, N., *J. Catal.*, 1990, **121**, 432.